Nanoscale

PAPER

View Article Online
View Journal | View Issue

Cite this: *Nanoscale*, 2016, **8**, 901

Mechanical strain effects on black phosphorus nanoresonators

Cui-Xia Wang,[e] Chao Zhang,[e,g] Jin-Wu Jiang,*[c] Harold S. Park*[d] and Timon Rabczuk*[a,b,e,f]

Received 18th September 2015,
Accepted 10th November 2015

DOI: 10.1039/c5nr06441d

www.rsc.org/nanoscale

We perform classical molecular dynamics simulations to investigate the effects of mechanical strain on single-layer black phosphorus nanoresonators at different temperatures. We find that the resonant frequency is highly anisotropic in black phosphorus due to its intrinsic puckered configuration, and that the quality factor in the armchair direction is higher than in the zigzag direction at room temperature. The quality factors are also found to be intrinsically larger than those in graphene and MoS_2 nanoresonators. The quality factors can be increased by more than a factor of two by applying tensile strain, with uniaxial strain in the armchair direction being the most effective. However, there is an upper bound for the quality factor increase due to nonlinear effects at large strains, after which the quality factor decreases. The tension induced nonlinear effect is stronger along the zigzag direction, resulting in a smaller maximum strain for quality factor enhancement.

Black phosphorus (BP) is a new two-dimensional nanomaterial that is composed of atomic layers of phosphorus stacked *via* van der Waals forces.[1] BP has a number of unique properties unavailable in other two-dimensional crystal materials. For example, BP has anisotropic properties due to its puckered configuration.[2–5]

While most existing experiments have focused on the potential electronic applications of BP,[6–8] a recent experiment showed that the resonant vibration response of BP resonators (BPRs) can be achieved at a very high frequency.[9] However, there have been no theoretical studies on intrinsic dissipation in BPRs to-date. In particular, it is interesting and important to characterize the effects of mechanical strain on the quality (Q)-factors of BPRs given their anisotropic crystal structure, and furthermore considering that mechanical strain can act as an efficient tool to manipulate various physical properties in the BP structure.[10–17] For example, a large uniaxial strain in the direction normal to the SLBP plane can even induce a semiconductor-metal transition.[18–21] We thus investigate the mechanical strain effect on the BPRs in armchair and zigzag directions, at different temperatures.

In this work, we examine the effect of mechanical tension on a single-layer BPR (SLBPR) *via* classical molecular dynamics (MD) simulations. Both uniaxial and biaxial tension are found to increase the quality factor of the SLBPR, as the resonant frequency is enhanced by the applied tension. However, the Q-factor decreases beyond a critical strain value due to the introduction of nonlinear energy dissipation, which becomes dominant at large tensile strains. As a result, there is a critical strain at which the quality factor reaches a maximum value, which is about 4% and 8% at 50 K for mechanical tension along the zigzag and armchair directions, respectively. We find that nonlinear dissipation is stronger if the BPR is stretched along the zigzag direction, which results in a smaller critical strain.

Fig. 1 shows the structure of SLBP with a dimension of 50 × 50 Å that is used in our simulations. The atomic interactions are described by a recently-developed Stillinger–Weber potential.[22] In the development of the Stillinger–Weber potential, all geometrical parameters in the Stillinger–Weber potential are determined analytically according to the equilibrium conditions for each individual potential term, while the energy parameters are derived from the valence force field model. In doing so, the accuracy of the valence force field model is transferred to the Stillinger–Weber potential. This Stillinger–Weber potential gives accurate linear properties, which have been

[a]*Division of Computational Mechanics, Ton Duc Thang University, Ho Chi Minh City, Vietnam. E-mail: timon.rabczuk@tdt.edu.vn*
[b]*Faculty of Civil Engineering, Ton Duc Thang University, Ho Chi Minh City, Vietnam*
[c]*Shanghai Institute of Applied Mathematics and Mechanics, Shanghai Key Laboratory of Mechanics in Energy Engineering, Shanghai University, Shanghai 200072, People's Republic of China. E-mail: jwjiang5918@hotmail.com*
[d]*Department of Mechanical Engineering, Boston University, Boston, Massachusetts 02215, USA. E-mail: parkhs@bu.edu*
[e]*Institute of Structural Mechanics, Bauhaus-University Weimar, 99423 Weimar, Germany. E-mail: chao.zhang.weimar@gmail.com*
[f]*School of Civil, Environmental and Architectural Engineering, Korea University, 136-701 Korea*
[g]*College of Water Resources and Architectural Engineering, Northwest A&F University, 712100 Yangling, P.R. China*

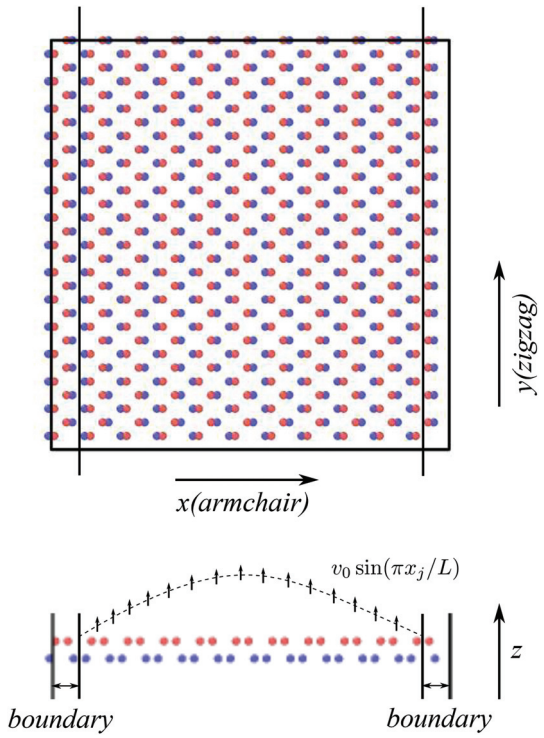

Fig. 1 Configuration of SLBP with the dimensions of 50 × 50 Å, from the top view in the top panel, and from the side view in the bottom panel. The total number of atoms is 660. Arrows in the bottom image indicate the direction of actuation.

shown to be comparable to first-principles calculations. In particular, phonon dispersion computed from the Stillinger–Weber potential agrees quite well with the first-principles calculations. The resonant oscillation of the SLBP resonator follows the lowest-frequency phonon branch (flexural mode) in SLBP. Hence, the linear properties (such as frequency) predicted in the present work are accurate. This Stillinger–Weber potential also yields accurate nonlinear properties. It is shown in the original reference that the stress–strain relation for the uniaxial tension of SLBP is accurate in the nonlinear deformation regime. As a result, the nonlinear properties (like the *Q*-factor) predicted in the present work should also be fairly accurate.

The BPR simulations are performed in the following manner. First, the entire system is thermalized to a constant temperature within the *NPT* (*i.e.*, the particle number N, the pressure P and the temperature T of the system are constant) ensemble by a Nosé–Hoover[23,24] thermostat, which is run for 200 ps. Second, SLBP is stretched by uniaxial or biaxial strain along the armchair or zigzag directions. Mechanical strain is applied at a strain rate of $\dot{\varepsilon} = 0.0001$ ps^{-1}, which is a typical value in MD simulations. Third, the configuration is divided into two parts as shown in Fig. 1, *i.e.*, the boundary part (2 × 5 Å) is fixed while the central part is actuated, as shown in the bottom panel of Fig. 1. The resonant oscillation of SLBP is actuated by adding a sine-shaped velocity distribution, $v_0 \sin(\pi x_j/L)$, to the system. In all simulations, we apply a velocity amplitude $v_0 = 2.0$ Å ps^{-1}, which is small enough to maintain resonant oscillation in the linear region. Fourth, the resonant oscillation of SLBP is simulated within the *NVE* (*i.e.*, the particle number N, the volume V and the energy E of the system are constant) ensemble for 90 ns, and the oscillation energy is recorded to extract the *Q*-factor.

We first examine the intrinsic energy dissipation of the SLBPRs along the armchair and zigzag directions. Intrinsic energy dissipation is induced by thermal vibrations at finite temperatures. We find that the oscillation amplitude of the kinetic energy decays gradually, which reflects energy dissipation during the resonant oscillation of the SLBPR. As the temperature increases, energy dissipation becomes stronger, indicating a lower *Q*-factor at higher temperature.

The frequency and the *Q*-factor of resonant oscillation can be extracted from the kinetic energy time history by fitting to the function $E_k(t) = \bar{E}_k + E_k^0 \cos(2\pi 2ft)\left(1 - \frac{2\pi}{Q}\right)^{ft}$. The first term $\bar{E}_k$ represents the average kinetic energy after resonant oscillation has completely decayed. The constant E_k^0 is the total kinetic energy at $t = 0$, *i.e.* at the moment when resonant oscillation is actuated. The frequency of resonant oscillation is f, so the frequency of the kinetic energy is $2f$. The kinetic energy time history is usually a very long data set, so it is almost impossible to fit it directly to the above function. The fitting procedure is thus done in the following two steps as shown in Fig. 2. First, Fig. 2(a) shows that the energy time history is fitted to the function $E_k(t) = \bar{E}_k + E_k^0 \cos(2\pi 2\, ft)$ in a very small time region $t \in [0, 50]$ ps, where the approximation of $\left(1 - \frac{2\pi}{Q}\right)^{ft} \approx 1$ has been used for the *Q*-factor term as energy dissipation is negligible in a small time range. The parameters E_k^0 and f are obtained from this step. Second, Fig. 2(b) shows that the oscillation amplitude of the kinetic energy can be fitted to the function $E_k^{amp}(t) = E_k^0\left(1 - \frac{2\pi}{Q}\right)^{ft}$ in the whole simulation range $t \in [0, 90]$ ns, which determines the *Q*-factor and $\bar{E}_k$. Following these fitting procedures, the *Q*-factor is 63 250 for the armchair SLBPR at 50 K.

Fig. 3 shows the temperature dependence for the *Q*-factor of the SLBPR along the armchair and zigzag directions. At most temperatures, the *Q*-factor is larger in the armchair direction. This means that the energy dissipation is weaker for the armchair SLBPR, considering that the frequency in the armchair SLBPR is only half of that in the zigzag SLBPR.[22] The temperature dependence for the *Q*-factor can be fitted to the functions $Q = 1.9 \times 10^7\ T^{-1.4}$ and $Q = 3.0 \times 10^6\ T^{-1.0}$ for the armchair and zigzag SLBPRs, respectively. We find that the *Q*-factor is in the order of 1000 at room temperature in our simulations, which is one order larger than the experimental value of 100.[9] In our numerical simulations, only the phonon–phonon scattering effect is included in determining the *Q*-factor of the black phosphorus resonator. In other words, we have investigated the intrinsic nonlinear effect as the energy dissipation mech-

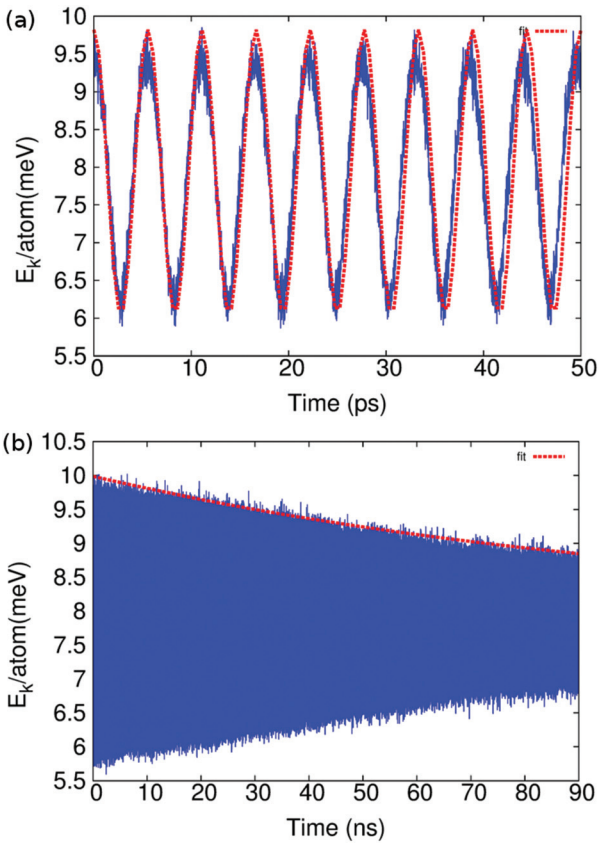

Fig. 2 Two-step fitting procedure to extract the frequency and Q-factor from the kinetic energy time history for the armchair SLBPR at 50 K. (a) The kinetic energy is fitted to the function $E_k(t) = \bar{E}_k + E_k^0 \cos(2\pi 2ft)$ in a small time range, giving a frequency of f = 0.090874 THz. (b) The kinetic energy is fitted to the function $E_k^{amp}(t) = E_k^0\left(1 - \frac{2\pi}{Q}\right)^{ft}$ in the whole time range, yielding the Q-factor value of 63 250.

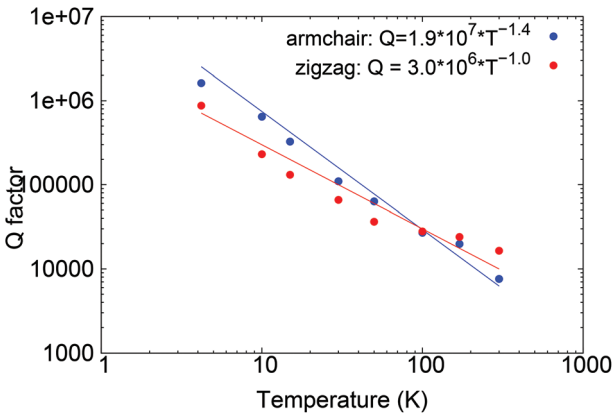

Fig. 3 Temperature dependence for the Q-factors of the armchair and zigzag SLBPRs.

anism for the resonator. However, there are many other energy dissipation mechanisms that could be introduced experimentally that are not accounted for in our simulations, *i.e.* ohmic losses, attachment losses, and two level systems.[25] Furthermore, black phosphorus is not stable under ambient conditions and defects could be present in the system. All of these factors could contribute to lowering the Q-factors for the experimental studies as compared to the pristine, defect-free system we have considered in our simulations.

These Q-factors are higher than the Q-factors in graphene nanoresonators ($Q = 7.8 \times 10^4\ T^{-1.2}$).[26,27] This is likely because there is also a large energy bandgap in the phonon dispersion of SLBP,[28] which helps to preserve the resonant oscillation of the SLBPR.[26] In contrast, there is no such energy bandgap in the phonon dispersion of graphene, so the SLBPR has a higher Q-factor than the graphene nanoresonators. The Q-factors of the SLBPRs are also higher than those of MoS_2 nanoresonators ($Q = 5.7 \times 10^5\ T^{-1.3}$).[26] Both SLBP and MoS_2 have energy bandgaps in their phonon dispersions. This is important as our simulation results imply that nonlinear phonon–phonon scattering is weaker in SLBP, *i.e.*, resonant energy dissipation is weaker in SLBP than MoS_2.

It is interesting to speculate how the Q-factors of multilayer black phosphorus would be compared to monolayer phosphorene. For multilayer black phosphorus, there are weak van der Waals interactions between individual phosphorene layers. The van der Waals interactions can reduce the Q-factors because they act as a frictional force between the layers, which provides an additional channel for the energy dissipation of the nanoresonators. Specifically, the strength of the interlayer van der Waals forces is likely to be the dominant factor in controlling the amount of energy that is dissipated, as was demonstrated for the case of multilayer graphene resonators by Kim and Park.[29]

We now report the effects of mechanical strain on both the armchair and zigzag SLBPRs at 50 K. We consider four cases, *i.e.*, (I) the effect of uniaxial strain on the armchair SLBPR, (II) the effect of uniaxial strain on the zigzag SLBPR, (III) the effect of biaxial strain on the armchair SLBPR, and (IV) the effect of biaxial strain on the zigzag SLBPR. Fig. 4 shows the strain

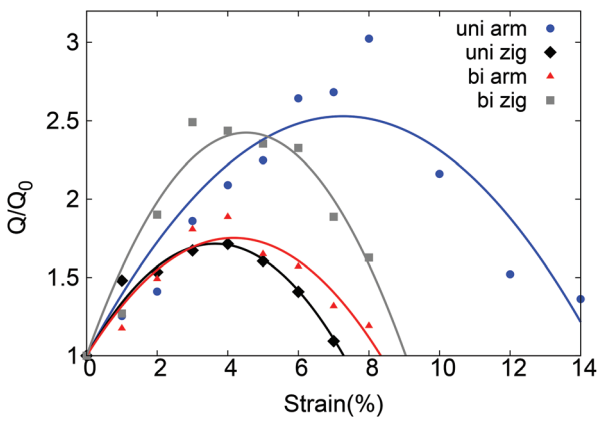

Fig. 4 Strain dependence for the Q-factor of the SLBPR in four cases at 50 K. The Q-factor depends on the strain as the function $Q/Q_0 = -a\varepsilon^2 + b\varepsilon + 1.0$, which gives a maximum Q-factor value at a critical strain.

dependence for the Q-factor (with reference to the value Q_0 without strain) of the SLBPRs under uniaxial or biaxial mechanical tension. In case I, the mechanical strain is applied purely in the armchair direction, while SLBP is stretched in the zigzag direction in the other three cases.

For all four cases, the Q-factor first increases and then decreases after a critical strain value. The Q-factor depends on the strain as the function $Q/Q_0 = -a\varepsilon^2 + b\varepsilon + 1.0$, where the fitting parameters (a, b) are (0.029, 0.42), (0.055, 0.40), (0.043, 0.36), and (0.070, 0.63) for the four studied cases. The linear term $b\varepsilon$ represents the enhancement effect on the Q-factor by mechanical tension, as the frequency of the resonator is increased by the tension in a small strain range. The quadratic term $-a\varepsilon^2$ is because the Q-factor will be reduced by the nonlinear effect resulting from the mechanical tension in a large strain range. The interplay between these two competing effects results in a maximum value for the Q-factor at a critical strain ε_c. The critical strain value is about 8% for case I, in which the mechanical tension is applied only in the armchair direction. For all other three cases, the critical strain is around 4%, where the mechanical tension has a component in the zigzag direction. It is clear that Q-factor reduction due to increased dissipation at increased temperature dominates the enhancements in the Q-factor that are possible through mechanical strain. However, Fig. 4 shows that strain engineering can be utilized to further manipulate the Q-factor of the black phosphorus resonators at a given temperature.

The differences in the above critical strains can be understood from the different strain induced nonlinear properties in SLBP. Fig. 5 shows the stress–strain curve for SLBP stretched in the above four cases. The stress–strain curve is fitted to the function $\sigma = E\varepsilon + \frac{1}{2}D\varepsilon^2$, with E as the Young's modulus and D as the third-order elastic constant (TOEC).[22] The nonlinear to linear ratio of $\gamma = \frac{\frac{1}{2}D}{E}$ gives an overall estimation of the strain induced nonlinear effect on SLBP. The parameter γ is found to be −1.66 for case I, −3.64 for case II and −3.65 for the other two cases. This means that the nonlinear effect is the weakest in case I, where SLBP is stretched purely in the armchair direction. As a result, the parameter a has the smallest value for case I, leading to the largest critical strain. This phenomenon (a maximum Q factor due to the strain effect) has also been obtained in nanowire resonators. For example, Kim and Park found that the maximum Q factor occurs at around 1.5% tensile strain in the metal nanowire resonators.[30] Very recently, several different possible stable two dimensional crystal structures were proposed for phosphorene.[31–33] We believe that similar nonlinear mechanical properties will be found in all of these phosphorene allotropes.

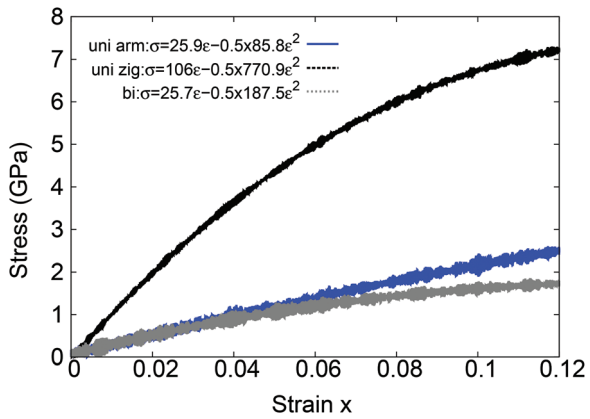

Fig. 5 Stress–strain relation for SLBP under mechanical tension. The stress (σ) is fitted to a function of the strain (ε) as $\sigma = E\varepsilon + \frac{1}{2}D\varepsilon^2$, with E as the Young's modulus and D as the TOEC. The nonlinear effect is estimated by the ratio $\gamma = \frac{\frac{1}{2}D}{E}\varepsilon$.

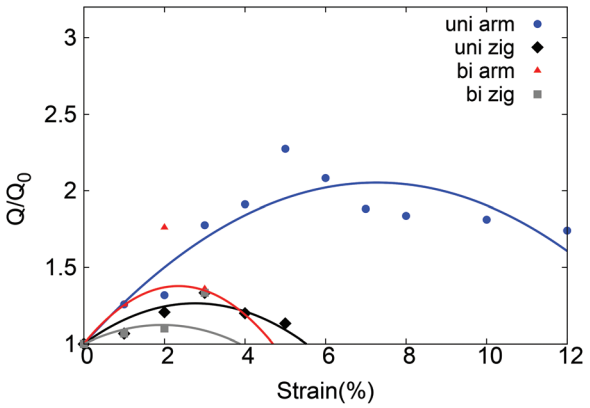

Fig. 6 Strain dependence for the Q-factor of the SLBPR in four cases at 170 K.

Fig. 6 shows the strain effect on the Q-factor at 170 K for all four cases. The critical strain is also observed at this higher temperature, and the critical strain value for the SLBR at 170 K is about 5% for case I and around 2–3% for the other three cases. However, the critical strain value is smaller as compared with the critical strain at 50 K in Fig. 4. This is because the nonlinear effect is stronger at higher temperature due to thermally-induced random vibrations. The combination of the two nonlinear effects (induced by temperature and strain) leads to a smaller critical strain at higher temperature.

In conclusion, we have performed classical molecular dynamics simulations to study the effects of mechanical tension on SLBPRs at different temperatures. We find that intrinsically, or neglecting strain, the Q-factors for an armchair SLBPR are generally higher than for a zigzag SLBPR, and are also larger than those found previously in graphene and MoS_2 nanoresonators. When the effects of mechanical strain are considered, our key finding is that there is a maximum point in the strain dependence of the Q-factor due to the competition between enhancement at small strains and reduction due to nonlinear effects at large strains.

Acknowledgements

The work is supported by the China Scholarship Council (CXW and CZ). JWJ is supported by the Recruitment Program of Global Youth Experts of China, the National Natural Science Foundation of China (NSFC) under Grant No. 11504225, and the start-up funding from Shanghai University. HSP acknowledges the support of the Mechanical Engineering department at Boston University.

References

1 A. Brown and S. Rundqvist, *Acta Crystallogr.*, 1965, **19**, 684.
2 Y. Du, C. Ouyang, S. Shi and M. Lei, *J. Appl. Phys.*, 2010, **107**, 093718.
3 A. Rodin, A. Carvalho and A. C. Neto, *Phys. Rev. Lett.*, 2014, **112**, 176801.
4 T. Low, A. Rodin, A. Carvalho, Y. Jiang, H. Wang, F. Xia and A. Castro Neto, arXiv preprint arXiv:1404.4030, 2014.
5 M. Engel, M. Steiner and P. Avouris, *Nano Lett.*, 2014, **14**, 6414.
6 L. Li, Y. Yu, G. J. Ye, Q. Ge, X. Ou, H. Wu, D. Feng, X. H. Chen and Y. Zhang, *Nat. Nanotechnol.*, 2014, **9**, 372.
7 H. Liu, A. T. Neal, Z. Zhu, D. Tomnek and P. D. Ye, *ACS Nano*, 2014, **8**, 4033.
8 M. Buscema, D. J. Groenendijk, S. I. Blanter, G. A. Steele, H. S. van der Zant and A. Castellanos-Gomez, Preprint at http://arxiv.org/abs/1403.0565v1, 2014.
9 Z. Wang, H. Jia, X. Zheng, R. Yang, Z. Wang, G. Ye, X. Chen, J. Shan and P. X.-L. Feng, *Nanoscale*, 2015, **7**, 877.
10 Q. Wei and X. Peng, *Appl. Phys. Lett.*, 2014, **104**, 251915.
11 R. Fei and L. Yang, *Appl. Phys. Lett.*, 2014, **105**, 083120.
12 Z.-Y. Ong, Y. Cai, G. Zhang and Y.-W. Zhang, *J. Phys. Chem. C*, 2014, **118**, 25272.
13 B. Sa, Y.-L. Li, J. Qi, R. Ahuja and Z. Sun, *J. Phys. Chem. C*, 2014, **118**, 26560.
14 L. Kou, Y. Ma, S. C. Smith and C. Chen, Preprint at http://arxiv.org/abs/1412.7602v1.
15 H. Y. Lv, W. J. Lu, D. F. Shao and Y. P. Sun, *Phys. Rev. B: Condens. Matter*, 2014, **90**, 085433.
16 J.-W. Jiang and H. S. Park, *Nat. Commun.*, 2014, **5**, 4727.
17 Y. Cai, Q. Ke, G. Zhang, Y. P. Feng, V. B. Shenoy and Y.-W. Zhang, Preprint at http://arxiv.org/abs/1502.00375, 2015.
18 A. S. Rodin, A. Carvalho and A. H. C. Neto, *Phys. Rev. Lett.*, 2014, **112**, 176801.
19 X. Han, H. M. Stewart, S. A. Shevlin, C. R. A. Catlow and Z. X. Guo, *Nano Lett.*, 2014, **14**, 4607.
20 G. Qin, Z. Qin, S.-Y. Yue, H.-J. Cui, Q.-R. Zheng, Q.-B. Yan and G. Su, arXiv:1406.0261, 2014.
21 G. Q. Huang and Z. W. Xing, Preprint at http://arxiv.org/abs/1409.7284v1, 2014.
22 J.-W. Jiang, *Nanotechnology*, 2015, **26**, 315706.
23 S. Nose, *J. Chem. Phys.*, 1984, **81**, 511.
24 W. G. Hoover, *Phys. Rev. A*, 1985, **31**, 1695.
25 C. Seoanez, F. Guinea and A. C. Neto, *Phys. Rev. B: Condens. Matter*, 2007, **76**, 125427.
26 J.-W. Jiang, H. S. Park and T. Rabczuk, *Nanoscale*, 2014, **6**, 3618.
27 S. Y. Kim and H. S. Park, *Nano Lett.*, 2009, **9**, 969.
28 J.-W. Jiang, *Nanotechnology*, 2015, **26**, 055701.
29 S. Y. Kim and H. S. Park, *Appl. Phys. Lett.*, 2009, **94**, 101918.
30 S. Y. Kim and H. S. Park, *Phys. Rev. Lett.*, 2008, **101**, 215502.
31 Z. Zhu and D. Tománek, *Phys. Rev. Lett.*, 2014, **112**, 176802.
32 J. Guan, Z. Zhu and D. Tománek, *Phys. Rev. Lett.*, 2014, **113**, 046804.
33 M. Wu, H. Fu, L. Zhou, K. Yao and X. C. Zeng, *Nano Lett.*, 2015, **15**, 3557.